Multifunctional Tactile Sensors using MEMS Cantilevers

Masayuki Sohgawa

Niigata University
8050 Ikarashi 2-no-cho, Nishi-ku,
Niigata, Japan
+81-25-262-7819, sohgawa@eng.niigata-u.ac.jp

Abstract

A multifunctional tactile sensor which can detect approximation, contact, slipping, and surface texture of the target has been developed. The sensor is composed of multiple MEMS cantilevers fabricated on Si substrate embedded in PDMS, and can detect normal and shear forces. By indenting and sliding the sensor on the object surface, output depending on hardness, friction, and roughness, etc. can be obtained. Moreover, a function for detection of proximity was integrated monolithically through photo-sensitivity of Si substrate.

Keywords: MEMS, surface micromachining, cantilever, PDMS, tactile sensor, proximity sensing, surface texture measurement

Introduction

In late years, robots with skillful performance in nursing care of aged and automation in manufacturing, agriculture, etc. have attracted much attention [1,2]. To ensure safety and workability for these applications, robots should detect approximation, touch, and slip to work objects. However, current conventional sensors such as optical, sonic and pressure sensors remain insufficient for this purpose [3]. Tactile sensors are much useful to recognize contact condition for holding the object.

We have developed the miniature multi-axial tactile sensor which can detect normal and shear forces using micro-cantilevers with NiCr strain gauge film embedded in the elastomer [4-7]. This sensor can detect normal and shear forces simultaneously [5,8]. By indenting and sliding the tactile sensor on the object surface like human active touching, the output corresponding to surface texture of objects, including friction, roughness, hardness, and so on can be obtained [9-11]. The surface texture of various kinds of materials, including papers, cloths, leathers, and resins can be recognized by the principal component analysis using feature quantities extracted from the sensor outputs. Moreover, a function for detection of proximity was integrated monolithically with the tactile sensor through photo-sensitivity of Si substrate [12,13]. The proximity information is obtained from AC impedance change, which is caused by photo-absorption of Si wafer irradiated by a neighboring LED chip.

Structure and Fabrication of Tactile Sensor

A. Structure

Fig. 1 shows a schematic illustration of the tactile sensor. One tactile sensor element is composed of three cantilevers

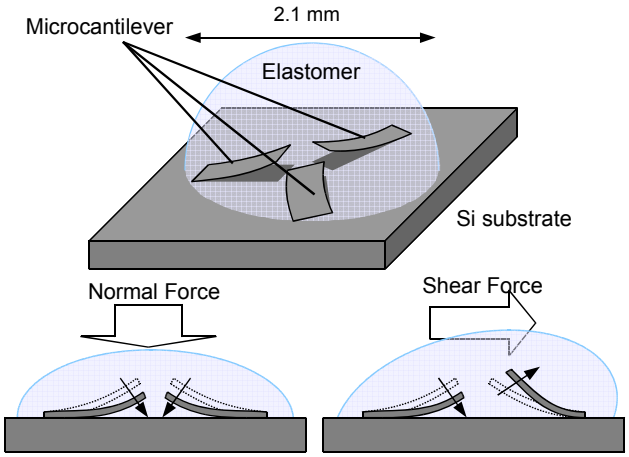

Fig. 1 A schematic illustration of the tactile sensor.

embedded in an elastomer. The cantilever has an inclined shape caused by residual stress in thin films formed on it so that it can deform both vertically and horizontally to the sensor surface. The thin-film strain gauge is set up on the cantilever to detect deformation of the cantilever. Deformation of the cantilevers is different from the direction of the applied force, so both normal and shear forces can be detected by this sensor [5,8].

B. Fabrication Process

A silicon-on-insulator (SOI) wafer was used as a substrate. At First, a Si_3N_4 thin film was deposited as an insulating layer. Then, a NiCr alloy thin film was deposited by the sputtering method. A Au/Cr layer was also formed as the electrode by the sputtering method. A Cr or a Cytop (Asahi Glass) thin film was used to bend the cantilever structure upward by residual stress in the thin film. Finally, the cantilever structure was formed by the sacrificial etching of the buried oxide layer in buffered hydrofluoric acid (BHF) solution for 5 h, and then dried in a vacuum chamber after rinsing in ultrapure water and then ethanol. The cantilevers were covered with hemispherical

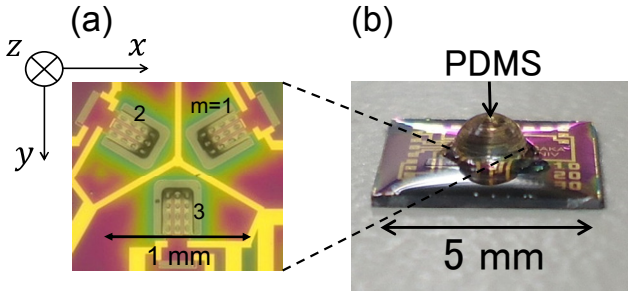

Fig. 2 A photograph of the fabricated tactile sensor.

PDMS (Silpot184; Toray Dow Corning). A photograph of the fabricated tactile sensor is shown in Fig. 2.

Detection of Normal and Shear Forces

The output voltage changes of the fabricated tactile sensor by applying of normal (f_z) and shear (f_x, f_y) forces are shown in Fig. 3 [6]. The output voltage changes increase with increasing of force intensity, and are almost linearly proportional to both the normal and shear forces with little hysteresis. Moreover, slope (sensitivity) of the output change of each cantilever depends on direction of the applied force. Therefore, it is demonstrated that intensity and direction of both normal and shear forces can be obtained from the output of the fabricated tactile sensor.

Characterization of Surface Texture

The output changes were measured when the tactile sensor was indented and slid on the object consisting of various materials including paper, cloth, leather, and resin [11]. Fig. 4 shows output (relative resistance changes) as a function of time by indention and slide of the sensor on the surface of foamed polystyrene and polyethylene terephthalate (PET). In the case of indentation of the sensor (Fig. 4(a)), the maximum change (indentation depth: 0.2 mm) depends on the hardness because polystyrene foam is softer than PET. In addition, the output change is asymmetric in indentation and pull-up tests because of relaxation of deformation in the case of polystyrene foam. On the other hand, in the case of sliding of the sensor, the output increases from 5 s because of the increase of the static friction force, as shown in Fig. 4(b). It is found that the increase of the output depends on the friction coefficient of the object. Moreover, the output periodically changes caused by surface roughness (polystyrene) and stick-slip oscillation (PET). From these results, hardness, thickness, friction, and surface roughness of the object can be characterized by the output change of the tactile sensor.

Multimodal Detection of Touch Force and Proximity

As described in previous sections, the micro-cantilever is deformed by touching of the target object, so that the resistance of the NiCr strain gauge is changed. On the other hand, the proximity is detected as the impedance change in Si by light intensity reflected from the object. A cross-sectional schematic view and equivalent circuit of the sensor are shown in Fig. 5. The touch force can be detected by measurement of DC resistance as the NiCr strain gauge (R_g). The impedance

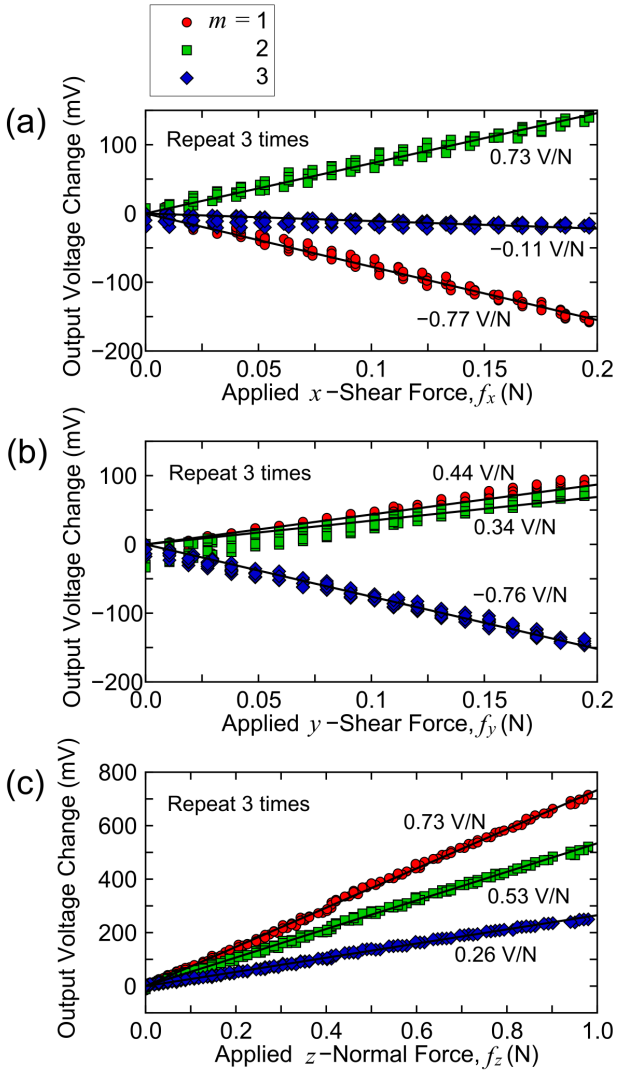

Fig. 3 Output voltage changes as a function of applied (a) x–shear, (b) y–shear and (c) z–normal forces [6].

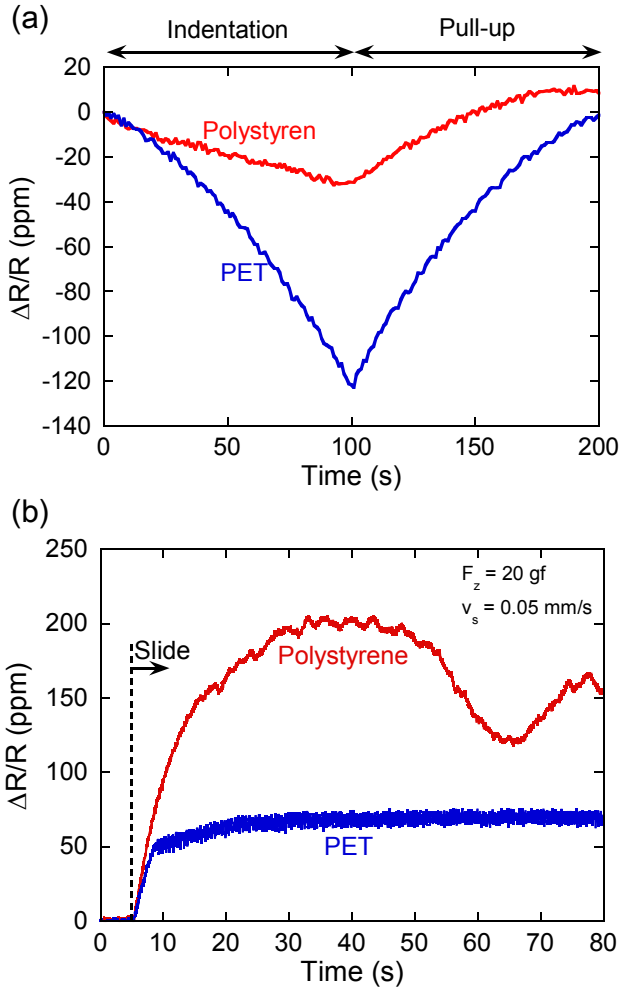

Fig. 4 Output changes of the tactile sensor as a function of time when the objects are (a) indented and (b) slid on the object surface.

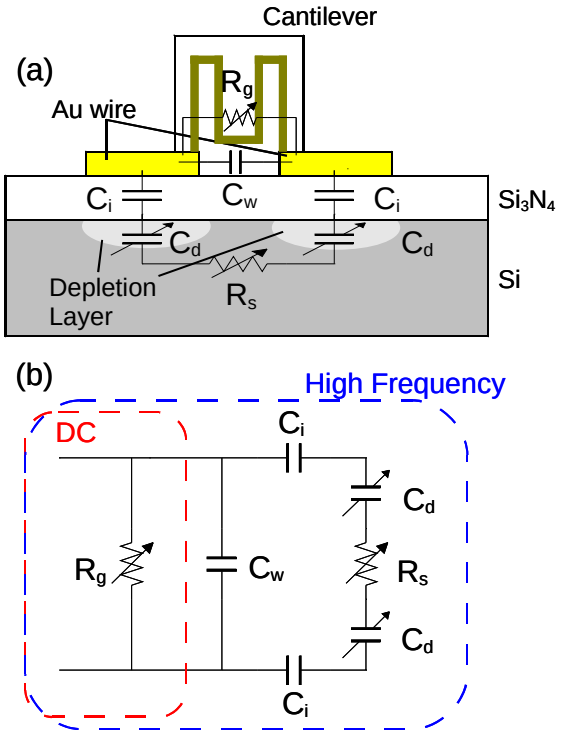

Fig. 5 (a) A cross-sectional schematic view of the sensor and (b) an equivalent circuit diagram of the sensor [12, 13].

measured at high frequency includes an electrical pathway through Si_3N_4 insulating layer and Si under Au electrodes as shown in Fig. 2 (a), so resistance (R_s) and capacitance of the depletion layer (C_d) depending on the photoconductive effect in Si can be measured through high-frequency AC impedance.

Fig. 6 shows DC resistance and AC impedance (at 1 MHz) change rates as a function of distance between the sensor surface and the object (PTFE board). A commercially available LED chip (5 mm x 5 mm) was employed as the probe light. The DC resistance is almost constant when the object do not contact with the sensor surface, but decreases linearly as a function depth of indentation. By contrast, the AC impedance increases with the saturated curve as a function of distance, because light intensity and photogenerated carrier in Si decreases in inverse proportion to the square of the distance. The shape of a concentric cylindrical object as shown in Fig. 7(a) was detected without touching [12]. Fig. 7(b) shows the impedance change rate (at 1 MHz) when the sensor is 2-dimensionally scanned on the cylindrical object from (x,y) = (0,0) to (75 mm, 75 mm). Fig. 7(c) shows the impedance change along x-axis at y = 37.5 mm. It is found that the cylindrical shape can be measured as the impedance change of the fabricated sensor.

Conclusion

A tactile sensor using MEMS cantilevers embedded in PDMS has been fabricated and characterized. The output of fabricated sensor is proportional to applied normal and shear forces with little hysteresis, and depends on the direction of the applied force. When the sensor is indented and slid on the various object surfaces, output depending on surface texture including hardness, thickness, friction, and roughness of the object is obtained. Moreover, the proximate information of the

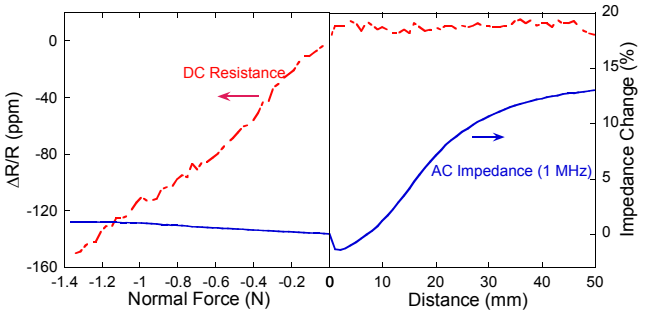

Fig. 6 DC resistance and AC impedance change rates as a function of distance between the sensor surface and the object (PTFE board).

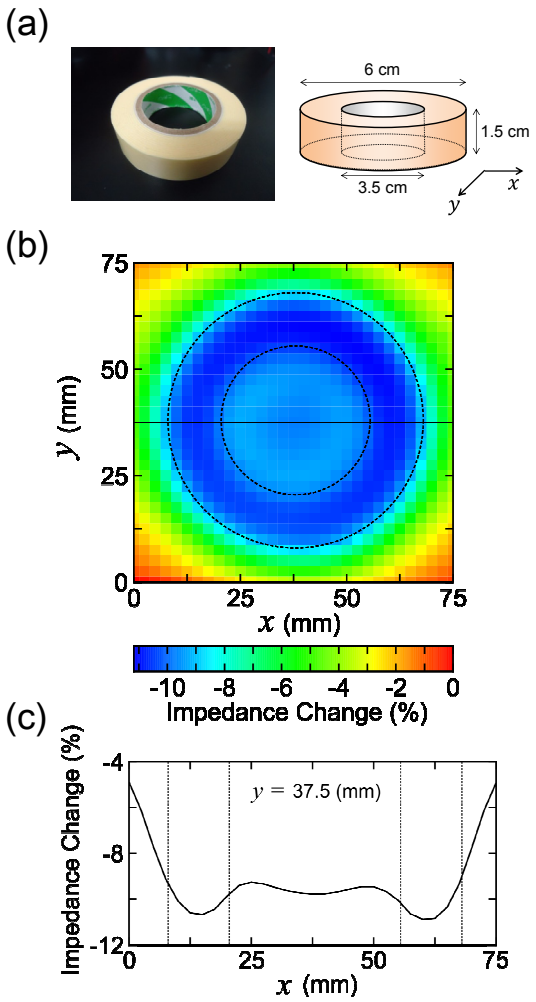

Fig. 7 DC resistance and AC impedance change rates as a function of distance between the sensor surface and the object (PTFE board) [12].

object can be detected by the high-frequency impedance measurement of the fabricated sensor because of the photoconductive effect in the substrate by reflected light from the object. Therefore, it is demonstrated that the fabricated sensor has ability to detect multimodal information of proximity, contact state, and surface texture of the object.

Acknowledgement

The author is grateful to Prof. Masanori Okuyama (Osaka

University), Prof. Haruo Noma (Ritsumeikan University), Dr. Teruaki Azuma (Nitta Corporation), and all other collaborators. This study was supported in part by Grants-in-Aid for Scientic Research (No. 25540069) from the Japan Society for the Promotion of Science, and a grant from Kanto Bureau of Economy, Trade and Industry, Japan.

References

[1] T. Mukai, M. Onishi, T. Odashima, S. Hirano, Z. Luo, *IEEE Trans. Robotics*, 24, pp. 505-512, 2008.

[2] M.I. Tiwana, S.J. Redmond, N.H. Lovell, *Sens. Actuators A*, 179, pp. 17–31, 2012

[3] R. S. Dahiya, G. Metta, M. Valle, G. Sandini, *IEEE Trans. Robotics*, 26, pp. 1-20, 2010.

[4] M. Sohgawa, T. Uematsu, W. Mito, T. Kanashima, M. Okuyama, H. Noma, *Jpn. J. Appl. Phys*, 50, 06GM08, 2011.

[5] M. Sohgawa, D. Hirashima, Y. Moriguchi, T. Uematsu, W. Mito, T. Kanashima, M. Okuyama, H. Noma, *Sens. Actuators A*, 186, pp. 32-37, 2012.

[6] H. Yokoyama, T. Kanashima, M. Okuyama, T. Abe, H. Noma, T. Azuma, M. Sohgawa, *IEEE Sensors 2013*, pp. 1090-1093, 2013.

[7] H. Yokoyama, T. Kanashima, M. Okuyama, T. Abe, H. Noma, T. Azuma, M. Sohgawa, *IEEJ Trans. Sensors Micromachines*, 134, pp. 58–63, 2014.

[8] H. Tachibana, S. Kamanaru, T. Mima, M. Sohgawa, T. Kanashima, M. Okuyama, K. Yamashita, M. Noda, H. Noma, M. Higuchi, *IEEJ Trans. Sensors Micromachines*, 130, pp. 223-229, 2010.

[9] K. Watanabe, M. Sohgawa, T. Kanashima, M. Okuyama, H. Noma, T. Azuma, *Transducers Eurosensors XXVII*, pp. 1012-1015. 2013.

[10] M. Sohgawa, K. Watanabe, T. Kanashima, M. Okuyama, H. Noma, T. Azuma, *IEEJ Trans. Sensors Micromachines*, 133, pp. 147-154, 2013.

[11] M. Sohgawa, K. Watanabe, T. Kanashima, M. Okuyama, H. Noma, T. Azuma, *IEEE Sensors 2014* (accepted).

[12] H. Yokoyama, T. Kanashima, M. Okuyama, T. Abe, H. Noma, T. Azuma, M. Sohgawa, *IEEJ Trans. Sensors Micromachines*, 134, pp. 229–234, 2014.

[13] M. Sohgawa, A. Nozawa, H. Yokoyama, T. Kanashima, M. Okuyama, T. Abe, H. Noma, T. Azume, *IEEE Sensors 2014* (accepted).